Frequency-Domain Time-Reversal Precoding in Wideband MISO OFDM Communication Systems

Trung-Hien Nguyen, *Member, IEEE,* Mathieu Van Eeckhaute, Jean-François Determe, Jérôme Louveaux, Philippe De Doncker, and François Horlin, *Member, IEEE*

***Abstract*—Time reversal (TR) recently emerged as an interesting communication technology capable of providing a good spatio-temporal signal focusing effect. New generations of large-bandwidth devices with reduced cost leverage the use of TR wideband communication systems. TR can easily be integrated into an orthogonal frequency division multiplexing (OFDM) system by precoding the signal in the frequency domain. However, frequency-domain TR precoding in the literature has considered only the rate back-off factor (BOF) of one, which does not exploit the focusing property of TR. In this paper, we discuss how to properly implement different BOFs on the OFDM system using frequency-domain TR precoding. Moreover, we demonstrate that increasing the BOF and/or the number of transmit antennas significantly improves the focusing gain at the intended position. In contrast, the un-intended position receives less useful power. Furthermore, a closed-form expression of the mean-square-error (MSE) of equalized received signals at the intended position is derived, demonstrating the focusing gain as a function of the BOF and the number of antennas. Numerical simulations with Rayleigh fading channels are carried out to validate the MSE expression.**

***Index Terms*—Time reversal, rate back-off factor, OFDM.**

I. Introduction

Time-reversal (TR) with sufficient rate back-off factor (BOF) has recently gained much attention as it can combine the energy from different multipath components to create a spatio-temporal focusing effect [1], [2]. TR precoding can be implemented in either time-domain (TD) or frequency-domain (FD). The TD/TR precoding has been well studied in the literature [2]. Because of the spatio-temporal focusing effect of TD/TR precoding systems, a one-tap equalizer is generally sufficient in such systems enabling a complexity reduction at the receiver.

Orthogonal frequency-division multiplexing (OFDM) is an efficient technology for the new generation wireless systems, thanks to its simple equalization of the frequency-selective channel. The FD/TR precoding combined with OFDM has been shown to be a simple and efficient technology [3]. However, the FD/TR precoding in the literature did not consider different BOFs and the impact of this parameter on the system performance, hence the advantage of TR was not exploited. For instance, in [3], the authors have derived the closed-form expression of the bit-error-rate (BER) of FD/TR precoding multiple-input single-output (MISO) OFDM systems with implicitly a BOF of one.

T.-H. Nguyen, M. Van Eeckhaute, J.-F. Determe, P. De Doncker, and F. Horlin are with OPERA department, Université libre de Bruxelles (ULB), 1050 Brussels, Belgium. E-mail: trung-hien.nguyen@ulb.ac.be

J. Louveaux is with ICTEAM institute, Université catholique de Louvain (UCL), 1348 Louvain-la-Neuve, Belgium.

Manuscript received Month XX, 2018; revised Month YY, 2018.

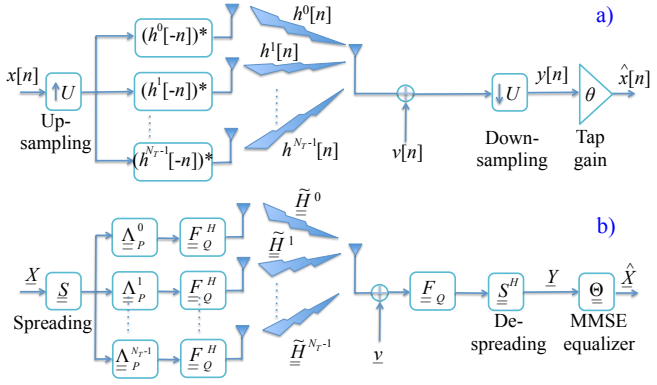

Fig. 1. Schematics of (a) the TD/TR precoding communication system [2] and (b) the corresponding FD/TR precoding OFDM system.

In this letter, we investigate for the first time the equivalent TR precoding method in the FD for MISO OFDM systems and assess the system performance with different BOFs in order to highlight the focusing gain given by the FD/TR precoding. We derive a closed-form mean square error (MSE) expression in the FD/TR precoding MISO OFDM systems at the intended position. More specifically, the MSE of the received symbols at the intended position is shown to be much less than that at the un-intended position, confirming the focusing gain of the FD/TR precoding. Numerical simulations are carried out to validate our analysis.

Notation: the underlined low-case and upper-case letters denote column vectors of TD and FD variables, respectively. Double-underlined upper-case letter corresponds to a matrix; $\underline{\underline{I}}_N$ is the $N \times N$ identity matrix; $\underline{\underline{F}}_Q$ is the $Q \times Q$ Fourier matrix; $|\cdot|$, $(\cdot)^*$, $(\cdot)^T$, $(\cdot)^H$ are the absolute, complex conjugate, transpose and Hermitian transpose operators, respectively; $\mathrm{tr}\{\cdot\}$ and $\mathbb{E}[\cdot]$ are the trace and expectation operators, respectively; $x!$ is the factorial of a positive integer x.

II. System Model

The TD/TR precoding MISO system is illustrated in Fig. 1(a) [2], where the TD symbol sequence $x[n]$ is firstly up-sampled by a BOF U and repeated on N_T transmit antenna branches. The signals are then pre-filtered by the TR precoder, $(h^k[-n])^*$, of the associated $k-$th channel impulse response (CIR), $h^k[n]$ before being sent over antennas. At the receiver side, the signal corrupted by additive white Gaussian noise

(AWGN) $v[n]$ is down-sampled by U. It is then equalized by a tap gain θ, which can be designed based on the minimum mean square error (MMSE) criterion. It has been shown in [2] that by using more antennas and/or increasing the BOF, the spatio-temporal focusing gain is improved accordingly, delivering a better bit-error-ratio (BER)/MSE performance.

In the literature, the performance of FD/TR precoding OFDM system was only assessed for a varying number of antennas [3], while the use of different BOFs has not been studied yet. We discuss here a proper way to assign the data symbols onto OFDM subcarriers in FD/TR precoding system, as illustrated in Fig. 1(b). The number of subcarriers of one OFDM symbol is Q. For simplicity, we consider that one OFDM symbol is sent over the TR precoding MISO OFDM system. We consider a transmit data vector $\underline{X}$ composed of N symbols X_n (for $n = 0, 1, ..., N-1$ with $N = Q/U$), i.e., $\underline{X} = [X_0 \ ... \ X_{N-1}]^T$. The symbol X_n is assumed to be an independent zero-mean random variable with variance $\mathbb{E}[|X_n|^2] = \sigma_X^2$. Without loss of generality, a normalized constellation is considered, i.e., $\sigma_X^2 = 1$.

The data symbols $\underline{X}$ are then spread by the matrix $\underline{\underline{S}}$ of size $Q \times N$. The matrix $\underline{\underline{S}}$ stacks U times $N \times N$ diagonal matrices, whose diagonal values are identically and independently distributed and taken from the set $\{\pm 1\}$. The spreading matrix is normalized by $\sqrt{U}$ in order to get $\underline{\underline{S}}^H \underline{\underline{S}} = \underline{\underline{I}}_N$. Thanks to the spreading matrix, the BOF discussed in the original TD/TR precoding is properly introduced. The idea behind this spreading comes from the fact that up-sampling a signal in the TD is equivalent to the repetition and shifting of its spectrum in the FD. Furthermore, the randomized spreading code is used to avoid assigning the same data symbol on OFDM subcarriers that causes a high peak-to-average-power ratio (PAPR) [4].

After spreading, the signal is repeated on N_T branches corresponding to transmit antennas and pre-coded by a matrix $\underline{\underline{\Lambda}}_P^k$ on each branch k. Defining $\underline{H}^k := [H_0^k \ H_1^k \ ... \ H_{Q-1}^k]^T$ as the channel frequency response (CFR) associated with the $k-$th antenna and assuming it is normalized such that $||\underline{H}^k|| = 1$, then $\underline{\underline{\Lambda}}_P^k$ is the diagonal matrix, whose diagonal element is $(H_q^k)^*$ (for $q = 0, 1, ..., Q-1$). The FD/TR precoding signals are transformed to the TD signals before being sent. The signal is then made cyclic by adding/removing a cyclic prefix (CP) and propagated over the channel, which is mathematically equivalent to the multiplication with the $Q \times Q$ circulant matrix $\underline{\underline{\widetilde{H}}}^k$ of the $k-$th CIR. The matrix $\underline{\underline{\widetilde{H}}}^k$ can be factorized as $\underline{\underline{\widetilde{H}}}^k = \underline{\underline{F}}_Q^H \cdot \underline{\underline{\Lambda}}_H^k \cdot \underline{\underline{F}}_Q$, where $\underline{\underline{\Lambda}}_H^k$ is the diagonal matrix, whose diagonal element stacks the element of vector $\underline{H}^k$. At the receiver, the reversed operations are carried out. Note that, the de-spreading operation reduces the symbol rate enabling the receiver to work at a *low-rate processing*. Assuming the time and frequency synchronization is perfect, the received signal after de-spreading is given by

$$\underline{Y} = \underline{\underline{S}}^H \cdot \underline{\underline{F}}_Q \cdot \left(\sum_{k=0}^{N_T-1} \underline{\underline{\widetilde{H}}}^k \cdot \underline{\underline{F}}_Q^H \cdot \underline{\underline{\Lambda}}_P^k \right) \cdot \underline{\underline{S}} \cdot \underline{X} + \underline{V}', \quad (1)$$

where $\underline{V}' = \underline{\underline{S}}^H \underline{\underline{F}}_Q \underline{v}$ is the equivalent FD circularly symmetric complex AWGN of the TD AWGN $\underline{v}$. We assume that the signal X_n and noise V_n' are independent of each other. We define the noise auto-correlation matrix as $\underline{\underline{R}}_{vv} := \mathbb{E}\left[\underline{v} \cdot \underline{v}^H\right] = \sigma_v^2 \underline{\underline{I}}_Q$, where σ_v^2 is the variance of $\underline{v}$. Based on the definition of the spreading matrix, we can deduce $\underline{\underline{R}}_{V'V'} = \sigma_v^2 \underline{\underline{I}}_N$. After some manipulations, (1) can be rewritten as $\underline{Y} = \underline{\underline{G}} \cdot \underline{X} + \underline{V}'$, where $\underline{\underline{G}} = \underline{\underline{S}}^H \cdot \left(\sum_{k=0}^{N_T-1} \underline{\underline{\Lambda}}_H^k \cdot \underline{\underline{\Lambda}}_P^k \right) \cdot \underline{\underline{S}}$.

Similarly to the TD/TR system, we use a one-tap MMSE equalizer after de-spreading in order to recover the transmitted signal. By multiplying $\underline{Y}$ with the MMSE equalizer matrix, calculated by $\underline{\underline{\Theta}} = \left(\underline{\underline{G}}^H \cdot \underline{\underline{G}} + \gamma^{-1} \underline{\underline{I}}_N \right)^{-1} \cdot \underline{\underline{G}}^H$ (in which $\gamma := \sigma_X^2 / \sigma_v^2$), we can obtain the estimate $\widehat{\underline{X}}$ of the input signal vector. It is worth noticing that if the TR precoding is matched to the channel, $\underline{\underline{\Theta}}$ is a real-valued diagonal matrix, leading to a *low-complexity equalizer* at the receiver.

III. Performance Assessment and Discussion

By defining $\underline{\varepsilon} := \underline{X} - \widehat{\underline{X}}$ and $\underline{\underline{R}}_{\varepsilon\varepsilon} := \mathbb{E}\left[\underline{\varepsilon} \cdot \underline{\varepsilon}^H\right]$, the MSE of the equalized received symbol can be derived as follows [5]

$$MSE = \mathrm{tr}\left\{ \underline{\underline{R}}_{\varepsilon\varepsilon} \right\} = \sigma_v^2 \cdot \mathrm{tr}\left\{ \mathbb{E}\left[\left(\underline{\underline{G}}^H \cdot \underline{\underline{G}} + \gamma^{-1} \underline{\underline{I}}_N \right)^{-1} \right] \right\}. \quad (2)$$

In order to assess the focusing gain of TR, we compare the normalized MSEs (NMSEs) (defined as $NMSE := MSE / \left(N \sigma_X^2 \right)$) of the received signal at both the intended and un-intended communication positions. Due to the fact that $\underline{\underline{G}}$ is the diagonal matrix, the NMSE is calculated by

$$NMSE = \mathbb{E}\left[\frac{\gamma^{-1}}{\frac{1}{U^2} K_n^2 + \gamma^{-1}} \right], \quad (3)$$

where K_n is a random variable (RV) depending on the channel realization. At the intended position, $K_n = \sum_{k=0}^{N_T-1} \sum_{u=0}^{U-1} \left| H_{n+uN}^k \right|^2$ and at the un-intended position, $K_n = \sum_{k=0}^{N_T-1} \sum_{u=0}^{U-1} \overline{H}_{n+uN}^k \cdot \left(H_{n+uN}^k \right)^*$, in which $\overline{H}_n^k$ is the $n-$th component of the un-intended position CFR associated with the $k-$th transmit antenna.

At the intended position: The RV K_n has the probability density function (PDF) $f_Z(z) = z^{M-1} \mathrm{e}^{-z} / (M-1)!$ [6], where $M = UN_T$. The derivation in the Appendix yields an approximation of (3) as the closed-form NMSE expression at the intended position (4), in which Γ_L and Γ_U are the lower and upper incomplete Gamma functions, respectively, and defined by

$$\Gamma_L(a, t) = \int_0^t x^{a-1} \mathrm{e}^{-x} dx, \quad (5)$$

$$\Gamma_U(a, t) = \int_t^\infty x^{a-1} \mathrm{e}^{-x} dx. \quad (6)$$

At the un-intended position: We assume that the CIRs between each transmit antenna and the receive antenna comprise no more than L taps and the CIRs are spatially independent. The variance of the l-th CIR tap is $\sigma_{h_l}^2 = \mathbb{E}\left[|h_l|^2 \right]$. Based on these assumptions, we observe that at the un-intended position the variable K_n^2 in (3) is constructed by the sum of

$$NMSE \approx \frac{1}{(UN_T-1)!}\left(\Gamma_L\left(UN_T, U\gamma^{-1/2}\right) - \frac{1}{U^2\gamma^{-1}}\Gamma_L\left(UN_T+2, U\gamma^{-1/2}\right) + \frac{1}{U^4\gamma^{-2}}\Gamma_L\left(UN_T+4, U\gamma^{-1/2}\right) + U^2\gamma^{-1}\Gamma_U\left(UN_T-2, U\gamma^{-1/2}\right) - U^4\gamma^{-2}\Gamma_U\left(UN_T-4, U\gamma^{-1/2}\right)\right). \quad (4)$$

correlated complex RVs, whose PDF (if existing) is difficult to derive. For example, the CFR correlation coefficient associated with the OFDM subcarriers p and q is [7] $\rho_{q-p} = \mathbb{E}\left[H_p H_q^*\right] = \sum_{l=0}^{L-1} \sigma_{h_l}^2 \exp\left(j2\pi\left(q-p\right)l/Q\right)$. We therefore evaluate the NMSE at the un-intended position numerically.

Discussion: Intuitively, the focusing gain is inversely proportional to the MSE. At the intended position, the RV K_n is built constructively thanks to the TR precoding of the signal with the corresponding CFR. This leads to the reduction of the NMSE and hence improves the focusing gain, especially when using a high number of antennas and BOFs. On the contrary, at the un-intended position, the RV K_n is constructed destructively from $(H_n^k)^*$ and $\overline{H}_n^k$ associated with the CFR component at the un-intended position, because of their spatial independence. This causes the increase in the NMSE in (3), especially when increasing the BOF and the number of antennas. Simulations will corroborate this observation.

Considering (4) at high signal-to-noise ratios (SNRs) to gain insight, we have $U\gamma^{-1/2} \approx 0$, $\Gamma_L\left(s, U\gamma^{-1/2}\right) \approx 0$ and in (4) the value of the fourth term is much bigger than that of the fifth term. The NMSE at high SNRs, $NMSE_h$, can be approximated by

$$NMSE_h \approx \frac{U^2\gamma^{-1}\Gamma\left(UN_T-2\right)}{(UN_T-1)!}, \quad (7)$$

where $\Gamma(a) = \Gamma_U(a,0)$ is the Gamma function. In the case a is a positive integer, $\Gamma(a) = (a-1)!$. Considering $UN_T > 2$, (7) is further simplified as follows

$$NMSE_h \approx \frac{\gamma^{-1}}{\left(N_T - 1/U\right)\left(N_T - 2/U\right)} \overset{U\to+\infty}{\to} \frac{\gamma^{-1}}{\left(N_T\right)^2}. \quad (8)$$

It reveals that when the BOF is sufficiently high, the NMSE can only be reduced by increasing the number of antennas, as shown later in the simulations. At low SNRs, the proposed NMSE approximation $NMSE_l$ is

$$NMSE_l \approx \frac{\Gamma_L\left(UN_T, U\gamma^{-1/2}\right)}{(UN_T-1)!}. \quad (9)$$

Using the series expansion of the lower incomplete Gamma function $\Gamma_L(a,t) = t^a\Gamma(a)\,\mathrm{e}^{-t}\sum_{k=0}^{\infty} t^k/\Gamma(a+k+1)$ [8] (equations (8.2.6) and (8.7.1)) and after some manipulations, we can obtain the following approximation

$$NMSE_l \approx 1 - \mathrm{e}^{-U\gamma^{-1/2}} \sum_{k=1}^{UN_T} \frac{\left(U\gamma^{-1/2}\right)^{UN_T-k}}{(UN_T-k)!}. \quad (10)$$

It can be seen that the same conclusion as for $NMSE_h$ can be drawn from (10). Considering a fixed value of N_T, the term $\mathrm{e}^{-U\gamma^{-1/2}}$ reduces faster than the summation term of (10) when increasing U, resulting in an un-changed $NMSE_l$ value if U is sufficiently high. In the case U is set to a certain value, $NMSE_l$ value can still be reduced further when increasing N_T as more terms are added in the summation. The accuracy of derived NMSE is evaluated in the next Section.

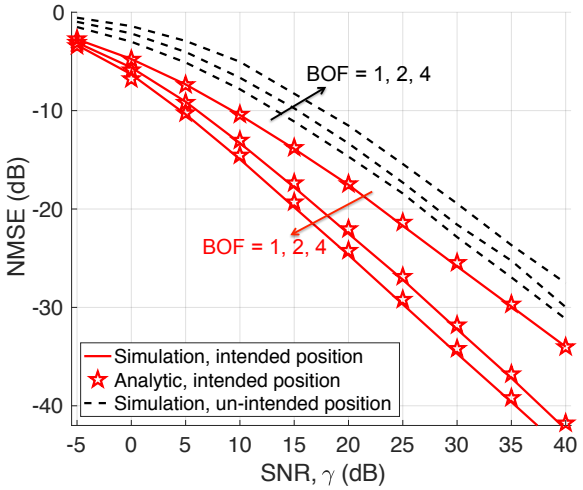

Fig. 2. NMSE versus SNR with different BOFs in the 2×1 MISO OFDM systems.

IV. Simulation Results

We consider a 256-subcarrier MISO OFDM system, i.e., $Q = 256$, and Rayleigh channels of 15 taps. The numerical results at the intended and un-intended positions are presented by the solid-lines and dashed-lines, respectively. The analytical results with respect to the intended position are plotted with marker symbols.

In the first step, we set the number of antennas to 2 and we plot NMSE versus SNR for different BOFs of 1, 2 and 4 in Fig. 2. As expected, at the intended position, the analytical closed-form NMSEs match the ones obtained by simulations, confirming the correctness of our derivation. The simulation results also confirm our previous observation that when increasing the BOF, the NMSE (and hence the spatio-temporal focusing) improves at the intended position; in contrast, it increases at the un-intended position.

In the second step, we set the SNR to 20 dB. We investigate the NMSE values when varying the number of antennas and BOFs. The results are presented in Fig. 3. At the intended position, as suggested in the analysis in Section III, the NMSE does not improve further when the BOF is sufficiently high. In this case, we can improve the NMSE by increasing the number of antennas. At the un-intended position, the NMSE worsens when the number of antennas and BOFs change from 1 to 16.

It should be noted that in the special case for which the number of antennas and the BOF are set equal to 1, the communication performance at the intended and un-intended positions is expected to be similar as there is no focusing

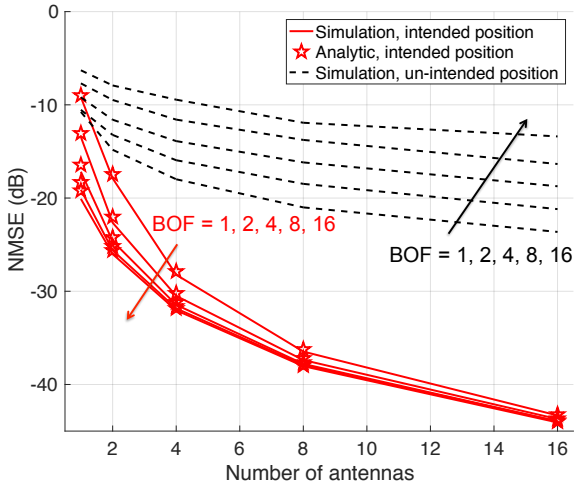

Fig. 3. NMSE of received symbols when using different number of antennas and BOFs. SNR = 20 dB.

gain and the MMSE equalization in both positions is similar. Surprisingly, we observe that the NMSE value at the un-intended position is smaller than that at the intended position (Fig. 3). It comes from the assumption of channel power normalization to one for each channel realization that is useful for the analytical derivation. However, whenever the number of antennas and/or the BOF are bigger than one, the focusing gain at the intended position is clearly visible.

V. Conclusion

We have presented a proper way to perform FD/TR precoding in MISO OFDM communication systems for BOFs different than one. By evaluating the NMSE, we have shown that, at the intended position, increasing either the BOF or the number of antennas improves the focusing gain. Conversely, at the un-intended position, the useful received power is lower. A closed-form NMSE approximation at the intended position has been derived and validated through simulations.

Appendix

At the intended position, based on the PDF of K_n, (3) can be rewritten as

$$\begin{aligned} NMSE &= \int_0^{\infty} \frac{\gamma^{-1}}{z^2/U^2+\gamma^{-1}} \frac{z^{M-1}}{(M-1)!}\mathrm{e}^{-z}dz \\ &= \frac{1}{(M-1)!}\left(\int_0^{U\gamma^{-1/2}} \frac{\gamma^{-1}}{z^2/U^2+\gamma^{-1}} z^{M-1}\mathrm{e}^{-z}dz + \right. \\ &\qquad \left. \int_{U\gamma^{-1/2}}^{\infty} \frac{\gamma^{-1}}{z^2/U^2+\gamma^{-1}} z^{M-1}\mathrm{e}^{-z}dz \right) \end{aligned} \tag{11}$$

Splitting the NMSE formula into two integrals $T_1 = \int_0^{U\gamma^{-1/2}} \frac{\gamma^{-1}}{z^2/U^2+\gamma^{-1}} z^{M-1}\mathrm{e}^{-z}dz$ and $T_2 = \int_{U\gamma^{-1/2}}^{\infty} \frac{\gamma^{-1}}{z^2/U^2+\gamma^{-1}} z^{M-1}\mathrm{e}^{-z}dz$ ensures that the integrals converge in the range of interest. More particularly, T_1 can be rewritten as

$$\begin{aligned} T_1 &= \int_0^{U\gamma^{-1/2}} \left(1+\tfrac{z^2}{U^2\gamma^{-1}}\right)^{-1} z^{M-1}\mathrm{e}^{-z}dz \\ &\approx \int_0^{U\gamma^{-1/2}} \left(1-\tfrac{z^2}{U^2\gamma^{-1}}+\tfrac{z^4}{U^4\gamma^{-2}}\right) z^{M-1}\mathrm{e}^{-z}dz \end{aligned}, \tag{12}$$

where the approximation is achieved by using the Taylor expansion $(1+x)^{-1} = \sum_{n=0}^{\infty}(-x)^n$ and the expansion converges since $z^2/\left(U^2\gamma^{-1}\right) < 1$ for $\forall z \in \left(0, U\gamma^{-1/2}\right)$. Substituting Γ_L defined in (5) into (12), we obtain the closed-form expression of T_1

$$\begin{aligned} T_1 \approx{}& \Gamma_L\left(M, U\gamma^{-1/2}\right) - \tfrac{1}{U^2\gamma^{-1}}\Gamma_L\left(M+2, U\gamma^{-1/2}\right) \\ &+ \tfrac{1}{U^4\gamma^{-2}}\Gamma_L\left(M+4, U\gamma^{-1/2}\right) \end{aligned}. \tag{13}$$

Due to the fact that $U^2\gamma^{-1}/z^2 < 1$ for $\forall z \in \left(U\gamma^{-1/2}, \infty\right)$, T_2 can be rewritten as follows

$$\begin{aligned} T_2 &= \int_{U\gamma^{-1/2}}^{\infty} U^2\gamma^{-1}z^{-2}\left(1+\tfrac{U^2\gamma^{-1}}{z^2}\right)^{-1} z^{M-1}\mathrm{e}^{-z}dz \\ &\approx \int_{U\gamma^{-1/2}}^{\infty} U^2\gamma^{-1}z^{-2}\left(1-\tfrac{U^2\gamma^{-1}}{z^2}\right) z^{M-1}\mathrm{e}^{-z}dz \end{aligned} \tag{14}$$

Using (6), the closed-form expression of T_2 can be derived

$$\begin{aligned} T_2 = U^2\gamma^{-1}&\Gamma_U\left(M-2, U\gamma^{-1/2}\right) \\ &- U^4\gamma^{-2}\Gamma_U\left(M-4, U\gamma^{-1/2}\right) \end{aligned} \tag{15}$$

Finally, substituting (13) and (15) into (11) and using the fact that $M = UN_T$, we achieve the closed-form NMSE expression at the intended position as in (4).

Acknowledgment

The authors would like to thank the financial support of the Copine-IoT Innoviris project, the Icity.Brussels project and the FEDER/EFRO grant.

References

[1] Y. Chen, Y.-H. Yang, F. Han, and K. J. R. Liu, "Time-reversal wideband communications," IEEE Signal Process. Lett., vol. 20, no. 12, pp. 1219–1222, Dec. 2013.

[2] M. Emami, M. Vu, J. Hansen, A. J. Paulraj, and G. Papanicolaou, "Matched filtering with rate back-off for low complexity communications in very large delay spread channels," Proc. Conf. Record 38th Asilomar Conf. Signals Syst. Comput., vol. 1, pp. 218–222, 2004.

[3] T. Dubois, M. Helard, M. Crussiere and C. Germond, "Performance of time reversal precoding technique for MISO-OFDM systems," EURASIP J. Wirel. Commun. Netw., article # 2013:260, 2013.

[4] M. Speth, S. Fechtel, G. Fock, and H. Meyr, "Optimum receiver design for wireless broad-band systems using OFDM - Part I," IEEE Trans. Commun., vol. 47, no. 11, pp. 1668–1677, Nov. 1999.

[5] A. Klein, G. K. Kaleh, and P. W. Baier, "Zero forcing and minimum mean-square-error equalization for multiuser detection in code-division multiple-access channels," IEEE Trans. Veh. Technol., vol. 45, no. 2, pp. 276–287, May 1996.

[6] A. Papoulis, "Probability, random variables and stochastic processes," McGraw-Hill Companies, 3rd edition, 1991.

[7] R. Hamila, O. Ozdemir, and N. Al-Dhabir, "Beamforming OFDM performance under joint phase noise and I/Q imbalance," IEEE Trans. Veh. Technol., vol. 65, no. 5, pp. 2978–2989, May 2016.

[8] NIST Digital Library of Mathematical Functions, link: https://dlmf.nist.gov/8.